Site-Selective Catalytic Surface Activation via Aerosol Nanoparticles for Use in Metal Micropatterning

Jeong Hoon Byeon,[†] Jae Hong Park,[†] Ki Young Yoon,[†] and Jungho Hwang*[,†,‡]

School of Mechanical Engineering and Yonsei Center for Clean Technology, Yonsei University, Seoul 120-749, Republic of Korea

Received February 15, 2008. Revised Manuscript Received March 14, 2008

There is great interest in the fabrication of micro- and nanopatterned metallic structures on substrates for a wide range of electronic, photonic, and magnetic devices. One of the most widely used techniques is the electroless deposition (ELD) of metal, which requires the surface activation of the substrates with a metal catalyst. This paper introduces a method of catalytic surface activation by producing platinum aerosol nanoparticles via spark generation and then thermophoretically depositing the particles onto a flexible polyimide (PI) substrate through the pattern hole of a mask. After annealing, the catalytically activated substrate is placed into a solution for electroless silver deposition. The silver is then formed only on the activated regions of the substrate. Silver line patterns having a width of 18 μm and a height of 1 μm are created with the ability to be effectively reproduced. The average value of the resistivities is approximately 6.8 $\mu\Omega\cdot$cm, which is almost comparable to the theoretical resistivity of bulk silver (1.6 $\mu\Omega\cdot$cm). Other silver micropatterns containing square dot array, line, line array, Y-branched line, and tapered line using different pattern masks are also demonstrated.

Introduction

There is great interest in the fabrication of micro- and nanopatterned metallic structures on substrates for a wide range of electronic, photonic, and magnetic devices, including semiconductor logic and memory devices, photovoltaic cells, displays, and magnetic storage.[1] The electroless deposition (ELD) of metal is a convenient, inexpensive metallization technique that works on nano- or microsized objects and can be used to pattern 2D and 3D structures.[2,3] Since ELD requires surface activation with a metal catalyst, such as palladium and platinum, many researchers have investigated ways to advance the activation by combining photochemical,[4] chemical,[5] imprinting,[1] and self-assembled block copolymer[6,7] tools in order to grow site-selective catalysts. Most of these methods are based on lithographic techniques;[8–10] recently, methods using laser,[11,12] ultraviolet (UV) ray,[13,14] plasma,[15] and ion beams[16] have been reported. Use of the above-mentioned activation techniques generally involves deposition of an inorganometallic or organometallic coating. However, there have been some problems reported relating to coating, removal, and incomplete decomposition of the precursor.[17,18] Furthermore, the equipment required to produce laser, UV, plasma, and ion beams are still quite expensive and frequently require a high-vacuum environment.[18,19]

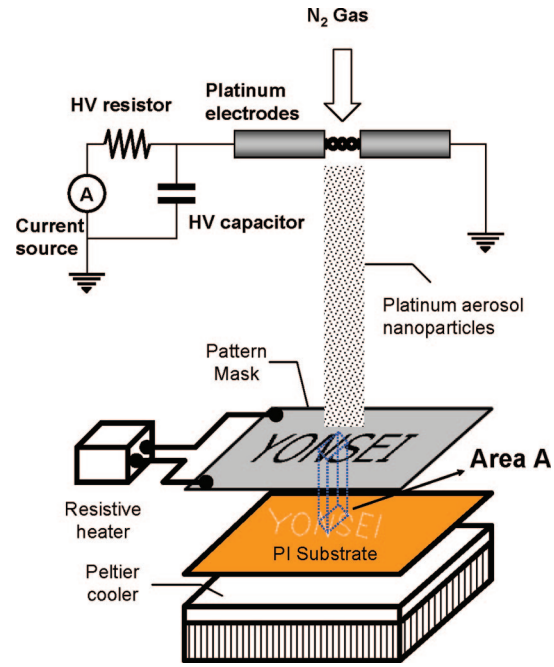

Figure 1. Overview of site-selective aerosol activation.

* To whom correspondence should be addressed. Phone:(+82-2) 2123-2821. Fax: (+82-2) 312-2821. E-mail: hwangjh@yonsei.ac.kr.
† School of Mechanical Engineering.
‡ Yonsei Center for Clean Technology.

(1) Hagberg, E. C.; Scott, J. C.; Shaw, J. A.; von Werne, T. A.; Maegerlein, J. A.; Carter, K. R. *Small* **2007**, *3*, 1703.
(2) Charbonnier, M.; Goepfert, Y.; Romand, M.; Leonard, D. *J. Adhes.* **2004**, *80*, 1103.
(3) Yanagimoto, H.; Deki, S.; Akamatsu, K.; Gotoh, K. *Thin Solid Films* **2005**, *491*, 18.
(4) Hozumi, A.; Asakura, S.; Fuwa, A.; Shirahata, N. *J. Vac. Sci. Technol. A* **2005**, *23*, 1029.
(5) Khoperia, T. N.; Tabatadze, T. J.; Zedgenidze, T. I. *Electrochim. Acta* **1997**, *42*, 3049.
(6) Xu, L.; Liao, J.; Huang, L.; Ou, D.; Guo, Z.; Zhang, H.; Ge, C.; Gu, N.; Liu, J. *Thin Solid Films* **2003**, *434*, 121.
(7) Sugimura, H.; Hanji, T.; Takai, O.; Masuda, T.; Misawa, H. *Electrochim. Acta* **2001**, *47*, 103.
(8) Zahl, P.; Bammerlin, M.; Meyer, G.; Schlittler, R. R. *Rev. Sci. Instrum.* **2005**, *76*, 023707−1.
(9) Dressick, W. J.; Dulcey, C. S.; Georger, J. H., Jr.; Calvert, J. M. *Chem. Mater.* **1993**, *5*, 148.
(10) Vargo, T. G.; Gardella, J. A., Jr.; Calvert, J. M.; Chen, M.-S. *Science* **1993**, *262*, 1711.
(11) Schrott, A. G.; Braren, B.; O'Sullivan, E. J. M.; Saraf, R. F.; Bailey, P.; Roldan, J. *J. Electrochem. Soc.* **1995**, *142*, 944.
(12) Chen, D.; Lu, Q.; Zhao, Y. *Appl. Surf. Sci.* **2006**, *253*, 1573.
(13) Zhang, J.-Y.; King, S. L.; Boyd, I. W.; Fang, Q. *Appl. Surf. Sci.* **1997**, *109*, 487.
(14) Esrom, H. *Appl. Surf. Sci.* **2000**, *168*, 1.
(15) Kreitz, S.; Penache, C.; Thomas, M.; Klages, C.-P. *Surf. Coat. Technol.* **2005**, *200*, 676.
(16) Weller, R. A.; Ryle, W. T.; Newton, A. T.; McMahon, M. D.; Miller, T. M.; Magruder, R. H., III *IEEE Trans. Nanotechnol.* **2003**, *2*, 154.
(17) Zhang, J.-Y.; Boyd, I. W. *Thin Solid Films* **1998**, *318*, 234.

10.1021/la8005019 CCC: $40.75
Published on Web 05/07/2008

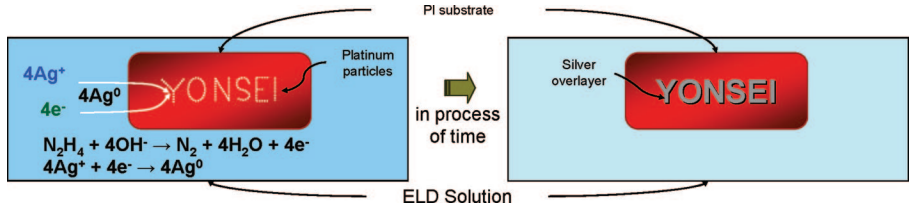

Figure 2. Schematic of silver ELD onto platinum pattern.

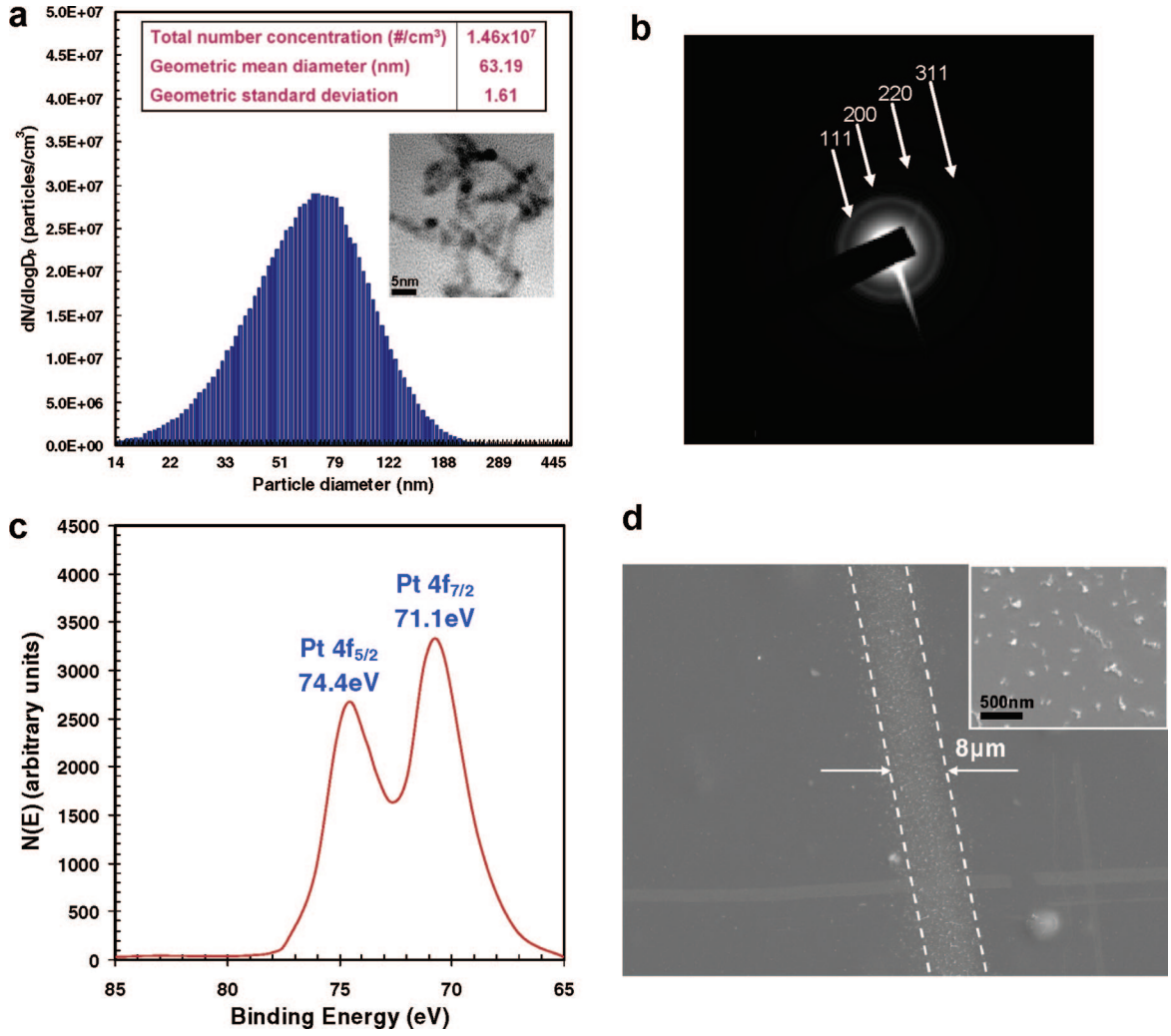

Figure 3. Particle characterization of aerosol activation. (a) Particle size distribution with a HRTEM image (inset) of spark-generated platinum particles. (b) SAED pattern of the particles. (c) XPS profile of the particles. (d) FESEM image of the pattern in the PI substrate.

Other surface activation processes include microcontact printing (μCP)[20–22] and inkjet printing (IJP);[23,24] these processes create patterned catalyst by directly stamping and jetting the catalyst, respectively. The key step in both μCP and IJP processes is the direct transfer of the catalyst from the stamp or nozzle to the substrate. However, a major challenge in applying a direct surface activation using μCP and IJP processes is the formulation of catalyst colloids. Two critical issues with colloids reside in the sedimentation stability of the corresponding colloids, which typically require stabilizers (binders, dispersants, and adhesion promoters), and limiting the metal concentration to low values.[23–25] Furthermore, there have also been other problems such as the ability to reproduce the colloidal pattern and washing of the colloids.

In this paper we introduce a strategy for catalytic surface activation by producing metal aerosol nanoparticles via spark generation. Spark generation has been used to produce particles of metals, alloys, and compounds for a wide range of materials having particle sizes ranging from several nanometers up to ~100 μm.[26,27] Our technique does not need any special devices such

(18) Zhang, J. Y.; Boyd, I. W. *Appl. Phys. A: Mater. Sci. Process.* **1997**, *65*, 379.
(19) Kordas, K.; Békési, J.; Bali, K.; Vajtai, R.; Nánai, L.; George, T. F.; Leppävuori, S. *J. Mater. Res.* **1999**, *14*, 3690.
(20) Hidber, P. C.; Helbig, W.; Kim, E.; Whitesides, G. M. *Langmuir* **1996**, *12*, 1375.
(21) Geissler, M.; Wolf, H.; Stutz, R.; Delamarche, E.; Grummt, U.-W.; Michel, B.; Bietsch, A. *Langmuir* **2003**, *19*, 6301.
(22) Hendricks, T. R.; Lee, I. *Thin Solid Films* **2006**, *515*, 2347.
(23) Shah, P.; Kevrekidis, Y.; Benziger, J. *Langmuir* **1999**, *15*, 1584.
(24) Cheng, K.; Yang, M.-H.; Chiu, W. W. W.; Huang, C.-Y.; Chang, J.; Ying, T.-F.; Yang, Y. *Macromol. Rapid Commun.* **2005**, *26*, 247.
(25) Busato, S.; Belloli, A.; Ermanni, P. *Sens. Actuators B* **2007**, *123*, 840.
(26) Schwyn, S.; Garwin, E.; Schmidt-Ott, A. *J. Aerosol Sci.* **1988**, *19*, 639.

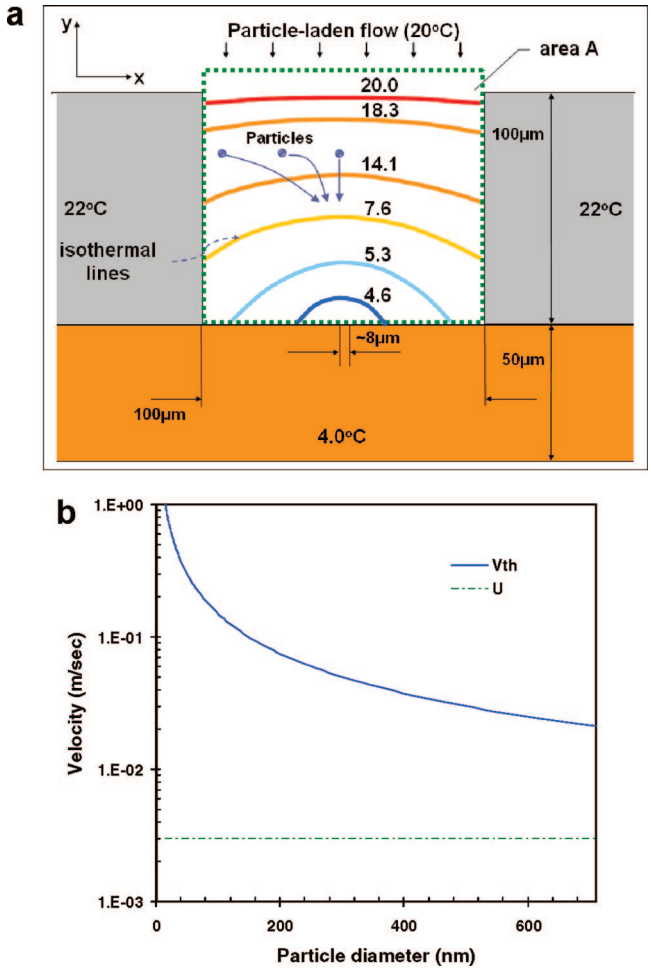

Figure 4. (a) Temperature distribution inside area A of Figure 1. (b) Thermophoretic velocity distribution as a function of particle size. *U* is the average upstream velocity of the particle-laden flow.

as laser, UV, plasma, and electron beams nor does it require special preparations such as catalyst colloid solutions. We enhanced the deposition of platinum aerosol particles onto a flexible polyimide (PI) substrate by controlling the thermophoresis, which is a physical phenomenon in which aerosol particles,[28–30] subjected to a temperature gradient, move from high- to low-temperature zones of the gas. Without any chemical pretreatment, we were able to reproduce a stable and selective deposition of particles on the PI substrate through a pattern hole. After annealing, the catalytically activated PI substrate was immersed in a silver ELD solution that resulted in the ELD of silver on the platinum nanoparticles of the PI substrate.

Experimental Section

Process. Figure 1 shows an overview of our surface activation. The platinum nanoparticles were generated via spark discharge and carried by N_2 gas to a PI substrate through the pattern hole (width, 100 μm; depth, 100 μm) of the "YONSEI" mask (Debora Electronics Co., Ltd., Korea) for a duration of 5 min. The mask was fabricated by a laser beam cutting technique. In our experiments, commercially available PI films (Kapton, Dupont) having a 50 μm thickness were used as the substrates. A spark was generated between two identical platinum rods (diameter, 3 mm; length, 100 mm) inside a reactor (volume, 42.8 cm^3) under a pure nitrogen environment (less than 10^{-4} impurities) at STP.[31] The flow rate of the nitrogen gas, which was controlled by a mass flow controller, was set at 100 mL/min. The electrical circuit specifications were as follows: resistance of 0.5 MΩ, capacitance of 10 nF, loading current of 2 mA, applied voltage of 2.8 kV, and frequency of 667 Hz. The spark channel raised the gas temperature within the channel above a critical value,[32] which is enough to sublimate part of the electrodes. Since the duration of each spark was very short (~1.5 ms) and the vapors were rapidly cooled after the spark, supersaturation was achieved and nanoparticles were formed by nucleation/condensation.

While the temperature of the particle-laden flow was kept at 20 °C, the temperatures of the stainless steel mask and PI substrate were kept at 22 (for preventing unwanted deposition of the particles onto the mask via thermophoresis) and 4 °C (for enhancing the deposition of the particles onto the PI substrate via thermophoresis) through the use of a resistive heater and a Peltier cooler, respectively. The PI substrate was then separated from the mask and annealed at 190 °C for 5 min in air to prevent detachment of the particles from the PI substrate. After annealing, the catalytically activated PI substrate was immersed into a silver ELD solution that resulted in the ELD of silver on the platinum nanoparticles of the PI substrate. The ELD of silver at 20 °C resulted in silver patterns appearing within 10 min. The schematic of silver ELD onto the platinum pattern is shown in Figure 2. The overall reactions are also described in Figure 2. Two solutions were mixed and used for the ELD solution. Solution A contained 2 g of $AgNO_3$, 60 g of Na_2-EDTA, 88 mL of isopropyl alcohol, 12 mL of acetic acid, and 400 mL of NH_4OH in 1 L of deionized water. Solution B contained 3 mL of hydrazine, 2 mL of mercerine, and 400 mL of ethyl alcohol in 1 L of deionized water. A 30 mL amount of Solution A and 30 mL of Solution B were mixed together, and the activated PI substrate was then immersed into the mixture at 20 °C. The PI substrate was rinsed with deionized water after it was removed from the ELD solution to remove the residual and then set aside to dry.

Instrumentation. The size distribution of the platinum aerosol particles was measured by a scanning mobility particle sizer (SMPS) system consisting of an electrostatic classifier (TSI 3081), a condensation particle counter (TSI 3025), and an aerosol charge neutralizer (NRD 2U500). The SMPS system was operated with a sample flow of 0.3 L/min, a sheath flow of 3 L/min, and a scan time of 180 s (measurement range between 13.8 and 723 nm). After the particles were sampled on a porous carbon-supported copper grid located on a polyamide membrane filter 20 cm downstream of the spark generator, the morphologies and microstructures of the platinum particles were analyzed using a high-resolution transmission electron microscope (HRTEM, JEM-3010) operated at 300 kV. Field emission scanning electron microscope (FESEM, JSM-6500F, JEOL, Japan) images and energy-dispersive X-ray (EDX, JED-2300, JEOL, Japan) profiles were obtained at an accelerating voltage of 15 kV. X-ray photoelectron spectroscopy (XPS) measurements were performed on a Kratos AXIS HIS spectrometer using a monochromatized Al Kα X-ray source (1486.6 eV photons) at a constant dwell time of 100 ms and a pass energy of 40 eV. The X-ray source was run at a power of 150 W (15 kV and 10 mA). The pressure in the analysis chamber was maintained under 10^{-8} Torr during the measurements. All binding energies (BEs) were referenced to the C 1s hydrocarbon peak at 284.6 eV. X-ray diffraction (XRD) studies of the silver patterns were carried out on a Rigaku RINT-2100 diffractometer equipped with a thin film attachment using Cu Kα radiation (40 kV, 40 mA). The 2θ angles ranged between 10° and 90° with a speed of 4°/min by step scanning at an interval of 0.08°. The crystallite size of silver was calculated from the XRD spectra in accordance with Scherrer's formula ($t = 0.9\lambda/(B \cos \theta)$). An atomic force microscope (AFM) was used for the topography of the patterns. Topographic images were recorded under ambient conditions using a multimode scanning probe microscope (SPM) connected to a NanoScope IIIa controller. For the high-resolution images, an E

(27) Watters, R. L., Jr.; DeVoe, J. R.; Shen, F. H.; Small, J. A.; Marinenko, R. B. *Anal. Chem.* **1989**, *61*, 1826.
(28) Messerer, A.; Niessner, R.; Pöschl, U. *J. Aerosol Sci* **2003**, *34*, 1009.
(29) Gonzalez, D.; Nasibulin, A. G.; Baklanov, A. M.; Shandakov, S. D.; Brown, D. P.; Queipo, P.; Kauppinen, E. I. *Aerosol Sci. Technol.* **2005**, *39*, 1064.
(30) Zheng, F. *Adv. Colloid Interface Sci.* **2002**, *97*, 255.
(31) Byeon, J. H.; Park, J. H.; Yoon, K. Y.; Ko, B. J.; Ji, J. H.; Hwang, J. *Carbon* **2006**, *44*, 2106.

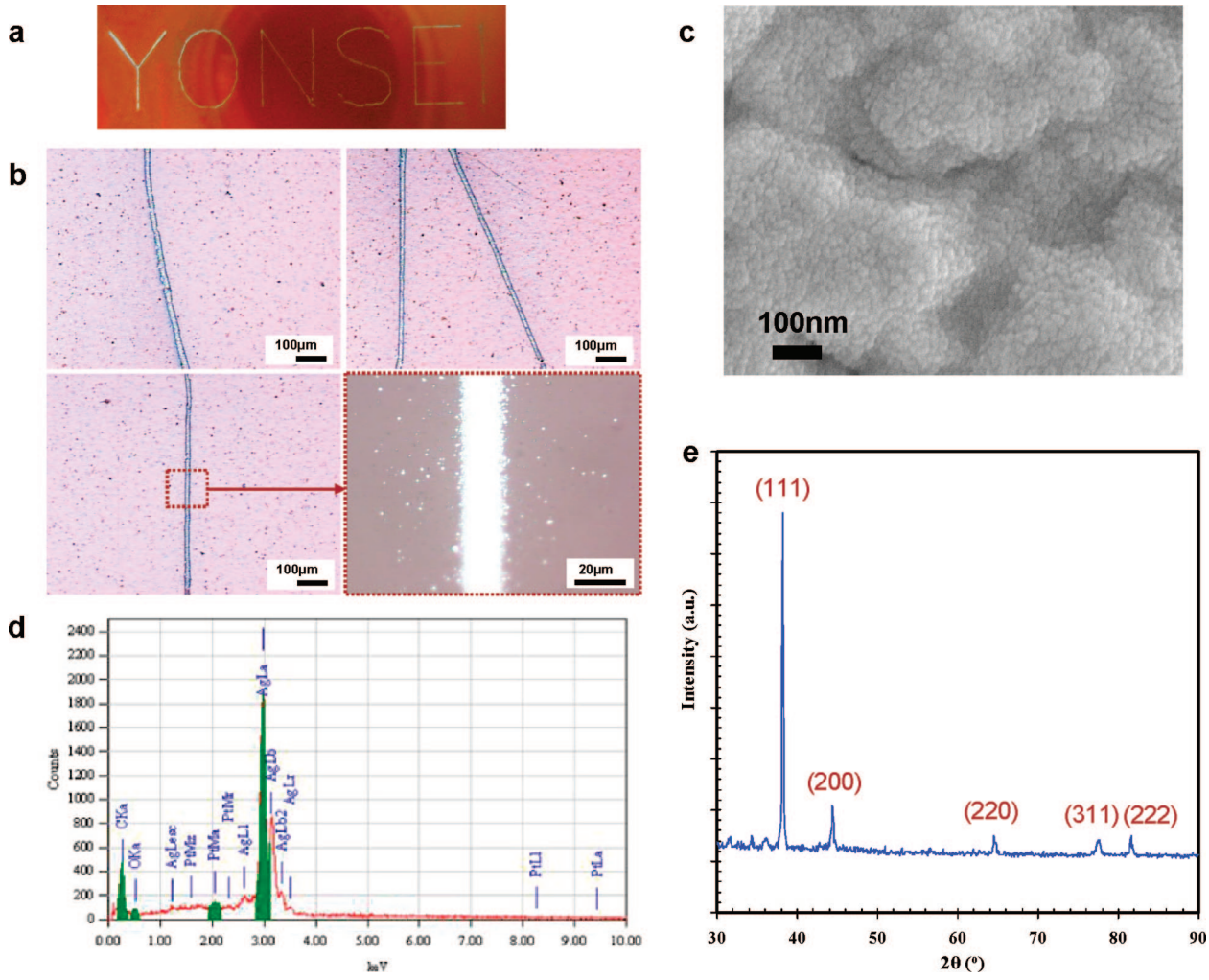

Figure 5. Results of silver ELD. (a) Photo of the silver pattern. (b) Optical microscopy images of the silver pattern. (c) FESEM micrograph corresponding to the optical microscopy images. (d) EDX profile. (e) XRD profile.

scanner having a maximum scanning size of 125 μm and a resolution of 0.2 Å was used. The SPM was operated in tapping mode, which allowed topography and phase contrast images to be recorded. The drive frequency was 330 kHz, and the voltage was between 3.0 and 4.0 V. The drive amplitude was about 300 mV, and the scan rate was 0.5−1.0 Hz. An arithmetic mean of the surface roughness was calculated from the roughness profile determined by the SPM. The resistances of the patterns were measured using a four-point probe (CMT-SR200N, Changmin Co., Ltd., Korea). The resistivities were calculated from the resistances and thicknesses of the patterns that were obtained by AFM observation. The $I-V$ measurements were performed in air using an Agilent 5263A source-measure unit.

Results and Discussion

The size distribution of the platinum nanoparticles was measured using a SMPS and is provided in Figure 3a. The electrical mobility diameter of the particles ranged from 20 to 200 nm. The morphology and structure of the particles were characterized by a HRTEM selected area electron diffraction (SAED) pattern and XPS. For the characterizations, the airborne particles were directly sampled on a porous carbon-coated copper grid. The HRTEM micrograph (inset of Figure 3a) reveals that the platinum particles were agglomerates of several primary particles (each ~26 Å in diameter). Figure 3b shows the SAED pattern corresponding to the HRTEM micrograph. The pattern has sharp diffraction lines showing [111] and [200] reflections and weak diffraction lines showing [220] and [311] of the face-centered cubic (fcc) lattice for metallic platinum. In addition, Figure 3c shows the XPS profile for the particles revealing that the particles were pure platinum. The binding energy (BE) doublet with the BEs for the Pt $4f_{7/2}$ and Pt $4f_{5/2}$ peak components lying

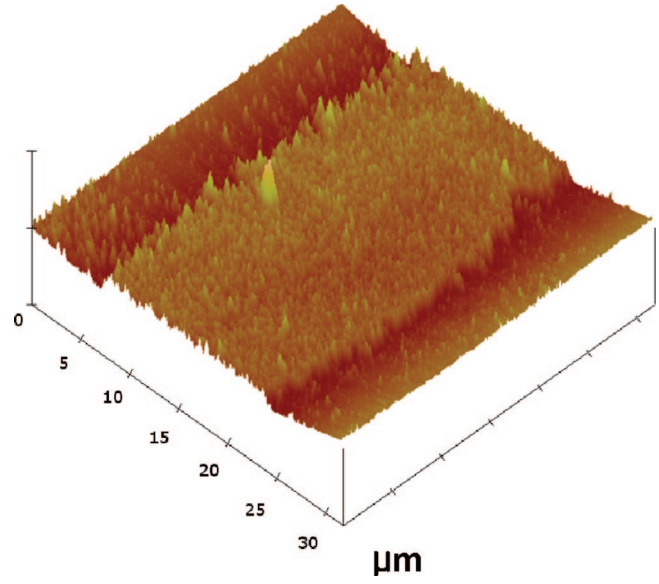

Figure 6. 3D Topograph of silver pattern.

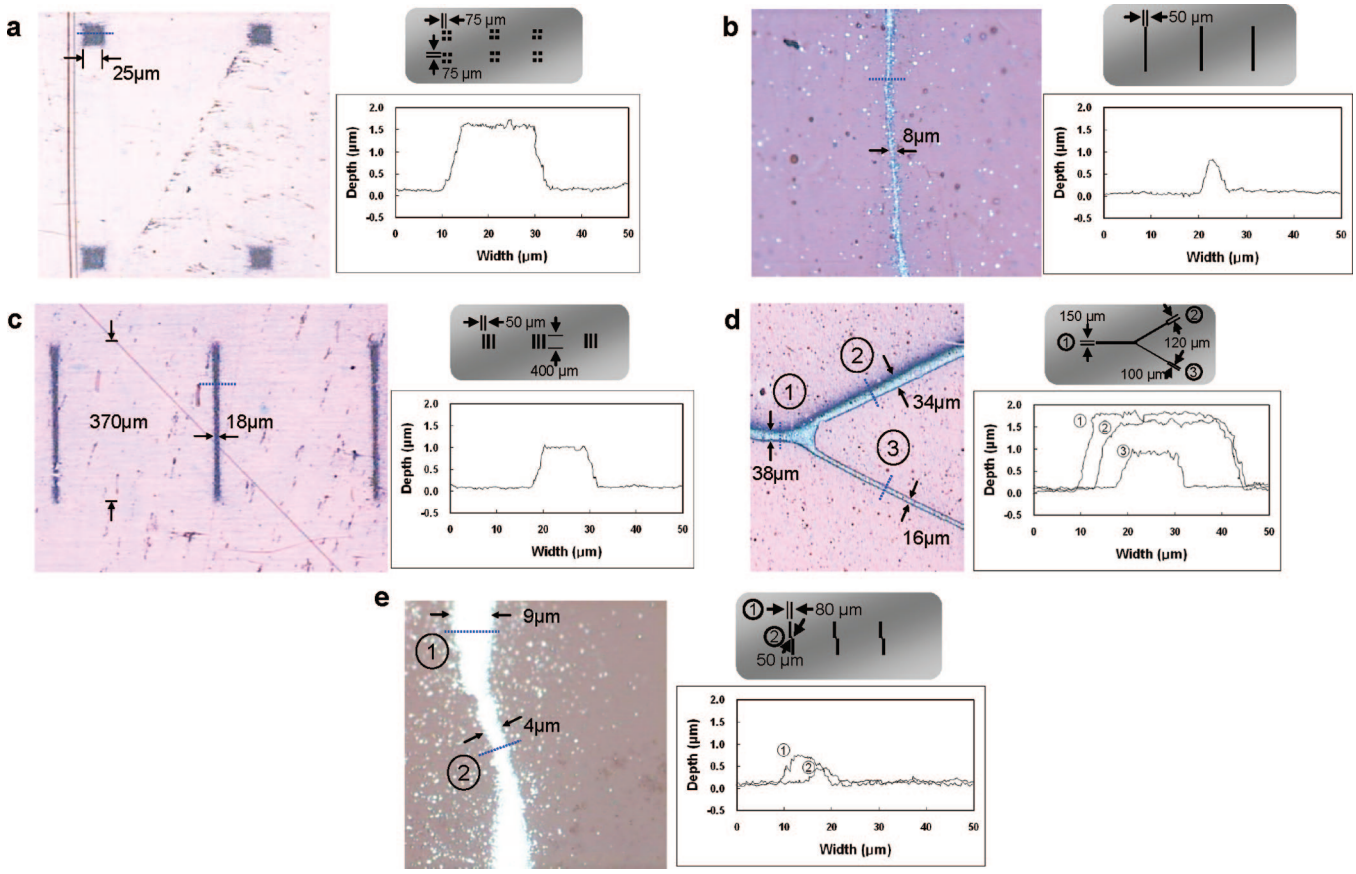

Figure 7. Optical microscope image, schematics of pattern mask, and cross-sectional profile for other silver micropatterns: (a) square dot array, (b) line, (c) line array, (d) Y-branched line, and (e) tapered line.

at about 71.1 and 74.4 eV, respectively, are assigned to the Pt^0 species.[33] Figure 3d shows a FESEM image of the particles in a line of the pattern. The FESEM image shows that the particles are spread out over the entire line. The FESEM image also shows that the thermophoretic focusing of the particles (see Figure 4a) resulted in a line width of ~8 μm, which is much narrower than the width of the hole (100 μm) in the mask.

To understand the effect of thermophoresis on particle deposition, velocities and temperatures of the particle-laden flow were calculated using a CFD code (Fluent 6.3) with a finite volume grid containing approximately 44 000 cells. Thermophoretic particle motion is usually described by the thermophoretic particle velocity

$$v_{th} = -K_{th}\frac{\mu_g \nabla T}{\rho_g T_p} \quad (1)$$

where ∇T represents the temperature gradient in the vicinity of the particle, μ_g is the gas dynamic viscosity, T_p the particle temperature, and ρ_g the gas density. K_{th} is the thermophoretic coefficient, which increases with decreasing particle size. As shown in Figure 4a, the particles were expected to be selectively deposited on the PI substrate by thermophoresis due to the temperature distribution inside the dotted area A. Figure 4b shows that thermophoretic *y*-direction velocities for all particles were higher than the average velocity of the particle-laden flow toward the mask.

Figure 5a shows a photo of the silver pattern. The optical microscopy analysis of Figure 5a revealed that line patterns having a width of 18 μm were obtained (Figure 5b). As shown in Figure 5b, the silver ELD occurred only on the platinum nanoparticles, i.e., at the activated region of the PI substrate. The platinum nanoparticles effectively acted as a seed to initiate the silver ELD. The line width of silver patterns (18 μm) was wider than that of platinum patterns (~8 μm, as shown in Figure 3d) because ELD is an isotropic process. A FESEM picture of a silver line pattern shows that silver particles were densely packed (Figure 5c). From the EDX analysis (Figure 5d) it was found that the coated metal consisted mainly of silver but contained a small amount of platinum as well as carbon and oxygen, which may have originated from the PI substrate. The XRD profile of the silver pattern shows that there exist five peaks located at 2θ = 38.2°, 44.4°, 64.5°, 77.5°, and 81.6° (Figure 5e). Compared with the data from the powder diffraction file No. 04-0783, these peaks correspond to the [111], [200], [220], [311], and [222] planes of the fcc phase for silver. The XRD profile shows the characteristics of pure metallic silver with a good crystallinity and without any impurity phase. The average particle size evaluated according to Scherrer's formula was approximately 35 nm.

AFM was used to determine the dimensions of the silver pattern. Figure 6 shows the 3D AFM profile obtained from Figure 5b. The height and root mean squared roughness were about 1 μm and 50 nm, respectively.

Resistivities (ρ) of the silver pattern were calculated through the relationship $\rho = RA/L$, where R, A, and L are the resistance, cross-sectional area, and length of the pattern, respectively. The average value of the resistivities was approximately 6.8 $\mu\Omega\cdot$cm, which is almost comparable to the theoretical resistivity of bulk silver (1.6 $\mu\Omega\cdot$cm).

(32) Berkowitz, A. E.; Walter, J. L. *J. Mater. Res.* **1987**, *2*, 277.
(33) Tian, Z. Q.; Jiang, S. P.; Liang, Y. M.; Shen, P. K. *J. Phy. Chem. B* **2006**, *110*, 5343.

Other silver micropatterns containing square dot array, line, line array, Y-branched line, and tapered line using different pattern masks were also demonstrated (Figure 7).

Using our site-selective aerosol activation and ELD processes it was possible to create stable and selective silver patterns with micrometer dimensions on a flexible PI substrate. Our processes were simple and environmentally benign and can be applied in order to produce display electronics circuits, sensors, radiofrequency identification (RFID) transponders, and other microelectronic devices.

Conclusions

This paper introduced a method of catalytic surface activation by producing platinum aerosol nanoparticles via spark generation and then thermophoretically depositing the particles onto a flexible PI substrate through the pattern hole of a mask. After annealing, the catalytically activated substrate was placed into a solution for silver ELD. The silver was then formed only on the activated regions of the substrate. Silver line patterns having a width of 18 μm and a height of 1 μm were created with the ability to be effectively reproduced. The average value of the resistivities was approximately 6.8 $\mu\Omega\cdot$cm, which was almost comparable to the theoretical resistivity of bulk silver (1.6 $\mu\Omega\cdot$cm). Other silver micropatterns containing square dot array, line, line array, Y-branched line, and tapered line using different pattern masks are also demonstrated.

Acknowledgment. This study was supported by a Korea Institute of Environmental Science and Technology Grant (2007-8-0368).

Supporting Information Available: Other silver micropatterns using different masks. This material is available free of charge via the Internet at http://pubs.acs.org.

LA8005019